Materials Letters 309 (2022) 131462

Contents lists available at ScienceDirect

Materials Letters

journal homepage: www.elsevier.com/locate/matlet

Processing of manganite-based contact layers for stacking of planar solid oxide fuel cells

E.A. Agarkova [a], D.V. Matveev [a], Yu. S. Fedotov [a], A.I. Ivanov [a], D.A. Agarkov [a,b,*], S. I. Bredikhin [a]

[a] Osipyan Institute of Solid State Physics RAS, 2 ul. Acad. Osipyana, Chernogolovka, Moscow District, 142432, Russia
[b] Moscow Institute of Physics and Technology, 9 Institutskiy per., Dolgoprudny, Moscow District, 141701, Russia

ARTICLE INFO

Keywords:
Planar SOFC
Contact materials
Current collection
LSM
Stability

ABSTRACT

Quality of the solid oxide fuel cell (SOFC) stack assembly affects power density and lifetime of the power plants. In the case of planar SOFCs, assembling quality depends on electrical contact between the stainless steel current collectors and ceramic electrodes of the membrane-electrode assemblies (MEAs). Whilst Ni meshes and paste are commonly used to provide this contact at the anode side, the cathode contact materials should be stable in oxidizing atmosphere. In this work, mechanical pre-treatment conditions of submicron $La_{0.8}Sr_{0.2}MnO_{3\pm\delta}$ (LSM) cathode powders were optimized in order to sinter mechanically stable contacts in the course of SOFC sealing procedure without use of inorganic sintering aids. Excessive ball-milling time and/or rotating speed was shown to result in partial decomposition of the perovskite phase, which increases electrical resistivity of the porous layers. Testing of the LSM contact layers in model SOFC stack with Crofer 22H current collectors under standard operating conditions demonstrated sufficient adhesion and performance.

1. Introduction

Electric power plants based on solid oxide fuel cells (SOFCs) provide environmentally friendly co-generation of the electricity and high-potential heat with minimum emissions, and are thus considered as a promising basis for power generation plants [1–3]. Conventional planar SOFC stacks consist of alternating membrane-electrode assemblies (MEA) and ferritic stainless steel current collectors with the gas flow channels [4–6]. In turn, MEAs are the multilayered ceramic plates comprising a gas-tight solid electrolyte membrane and porous anode and cathode; each functional MEA layer may also consist of several sublayers [5,7]. This architecture is illustrated in Fig. 1.

The interfaces between both electrodes and current collectors should have a low electrical resistivity and a sufficient stability in order to provide stack lifetimes of, at least, 30–50 thousands of hours [8,9]. At the anode side, good adhesion and electrical contact can be achieved by the application of metallic meshes [9]. The conditions inside the SOFC cathode chamber, primarily oxidizing atmosphere at elevated temperatures and high current densities, are more corrosive for metals such as stainless steel and nickel. This factor makes it necessary to apply non-metallic conductive layer at the cathode|current collector interface [10–12]. Respectively, development of the SOFC cathode contact materials is an important task for the stack elaboration and upscaling.

The present work was centered on processing of the contact layers made of lanthanum-strontium manganite (LSM), the conventional SOFC cathode component, without sintering aids and their testing for SOFC stacking.

2. Experimental section

Single-phase submicron powder of perovskite-type $La_{0.8}Sr_{0.2}MnO_{3\pm\delta}$ (LSM) was synthesized by the glycine-nitrate technique using high-purity $La(NO_3)_3\ 6H_2O$, $Sr(NO_3)_2$ and $Mn(CH_3COO)_2\ 4H_2O$ as starting materials [13]. The pre-final thermal treatment of the powder was carried out at 750 °C in air.

As-prepared LSM was ball-milled in ethanol using yttria-stabilized zirconia (YSZ) balls and planetary-type Pulverisette 6 instrument (Fritsch). Milling was performed for 300 and 500 min varying the rotation speed from 100 up to 600 rpm. Then LSM powder was dried and mixed with binder (9 wt% polyvinyl butyral - PVB, Butvar B-98, supplied by Acros Organics, USA), plasticizer (2 wt% diethyl adipate, Merck), dispersant (2 wt% diamine RRT, UPI Chem, USA), and solvent

* Corresponding author.
E-mail address: agarkov.da@mipt.ru (D.A. Agarkov).

https://doi.org/10.1016/j.matlet.2021.131462
Received 13 September 2021; Received in revised form 18 November 2021; Accepted 4 December 2021
Available online 9 December 2021

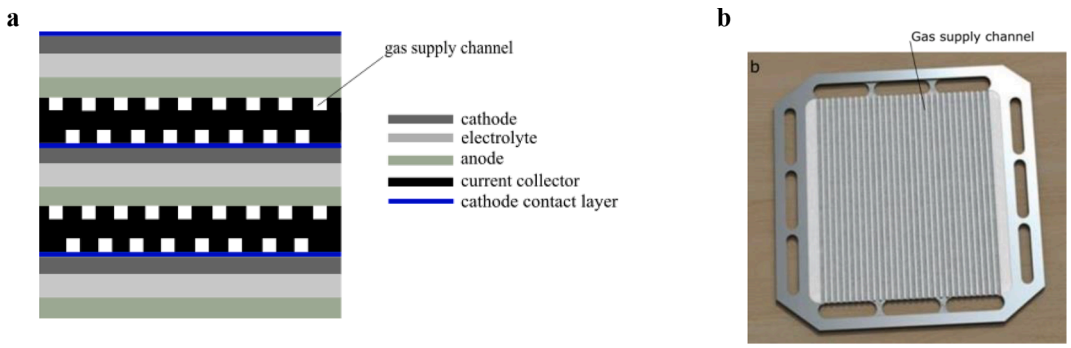

Fig.1. Schematic drawing of the planar SOFC stack architecture (a) and photo of the Crofer-22H stainless-steel bipolar plate with the gas supply channels (b).

Table 1
Results of XRD analysis and average particle sizes of as-synthesized and grinded powders.

Rotation speed (rpm)/ grinding time (min)	Particle size		Single phase preservation
	Agglomerates (SEM), μm	Grains (TEM), nm	
As-synthesized	5.8	110	+
100/300	18	65	+
100/500	12	31	+
200/300	20.4	58	+
200/500	3.6	42	+
550/300	6.2	33	–
550/500	13.6	27	–
600/300	2	30	–
600/500	2.4	33	–

(70:30 vol% mixture of toluene and butanol). The slurry was homogenized in a Thinky ARE-250 planetary mixer at a rotation speed of 600 rpm during 30 min.

Phase composition of the powders was studied by X-ray diffraction (XRD, Siemens D-500, $CuK_{\alpha 1}$ radiation). The powder morphology was characterized by the transmission electron microscopy (TEM, JEOL JEM-100CX). Microstructure of the contact layers prior to and after operation was assessed by the scanning electron microscopy (SEM, Supra 50 VP, Carl Zeiss). Thermogravimetric analysis (TGA) was performed using a Setaram Setsys Evolution 16/18 instrument in flowing air. Electrical resistivity of the LSM layers, similar to those tested in the SOFC stack and deposited onto YSZ ceramics under identical conditions, was measured by the 4-probe method at 600–950 °C on heating and subsequent cooling in air.

Performance of the manganite contact pastes was tested using a single SOFC unit sandwiched between two stainless-steel current collectors. The collectors shown in Fig. 1(b) were made of the Crofer 22H steel (ThyssenKrupp) with subsequent electrodeposition of protective Ni layers. The three-layer solid electrolyte membranes 6ScSZ/10Sc1YSZ/6ScSZ (6ScSZ: 6 mol% Sc_2O_3 stabilized ZrO_2; 10Sc1YSZ: 10 mol% Sc_2O_3 and 1 mol% Y_2O_3 co-stabilized ZrO_2) with the thickness of 150 μm and area of 10x10 cm^2 were produced by NEVZ-Ceramics (Russia). The anode comprised four layers, including $Ce_{0.8}Gd_{0.2}O_{2-\delta}$ (GDC) deposited directly onto the zirconia membrane, electrochemically active functional layer of NiO/GDC composite (50:50 wt%), current-collecting layer of NiO/10Sc1CeSZ composite (60:40 wt%; 10Sc1YSZ: 10 mol% Sc_2O_3 and 1 mol% CeO_2 co-stabilized ZrO_2), and the contact NiO layer. The cathode consisted of three layers made of GDC deposited onto the electrolyte, LSM/GDC (60:40 wt%) composite, and single-phase LSM. The multilayered electrodes were deposited by screen-printing [5,7] and then co-sintered at 1250 °C. The contact LSM paste was applied onto the sintered cathode. Following final assembling of the MEA, two current collectors and Ni mesh into the model stack, sealing was performed under the mechanical load of 0.4 kg/cm^2 at 940 °C. The electrochemical

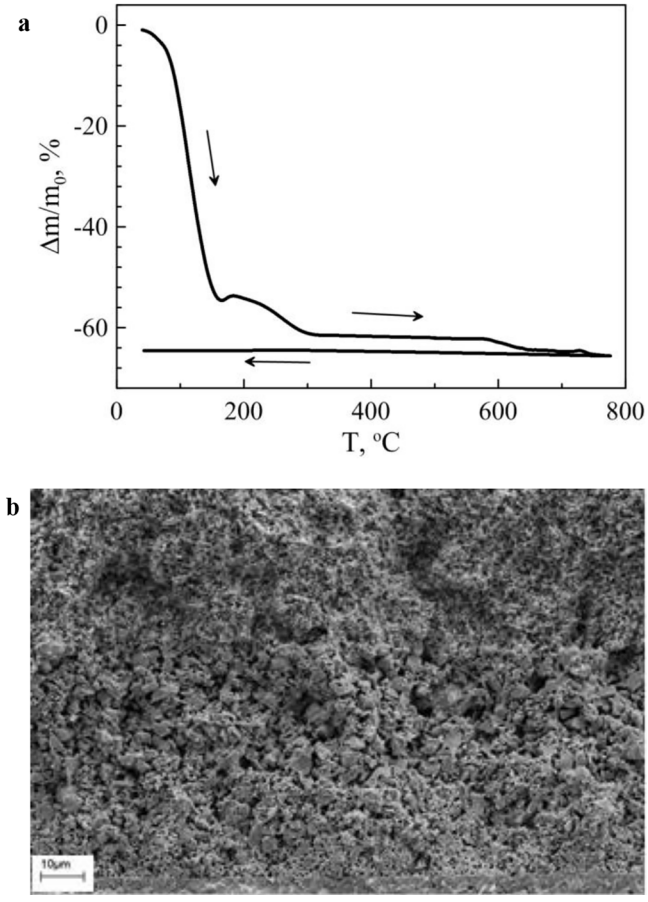

Fig.2. TGA curves of the manganite paste on heating and cooling in air (a), and typical microstructure of the LSM contact layer after SOFC tests (b).

measurements were carried out using a Reference 3000 potentiostat (Gamry, USA) equipped with an additional Reference 30 K Booster module. The tests were performed at 850 °C with 50% H_2 - 50% N_2 mixture as fuel and atmospheric air as oxidant.

3. Results and discussion

Selected results of XRD analysis and the average particle sizes, extracted by statistical treatment of the TEM and SEM data for as-synthesized and grinded LSM powders, are presented in Table 1and in the electronic Supporting Information. Briefly, grinding at 550 and 600 rpm led to partial LSM decomposition and an appearance of $Sr(OH)_2$ and $MnCO_3$ phases. The minimum grain size of single-phase powders was achieved after grinding at 200 rpm during 500 min. The LSM powder

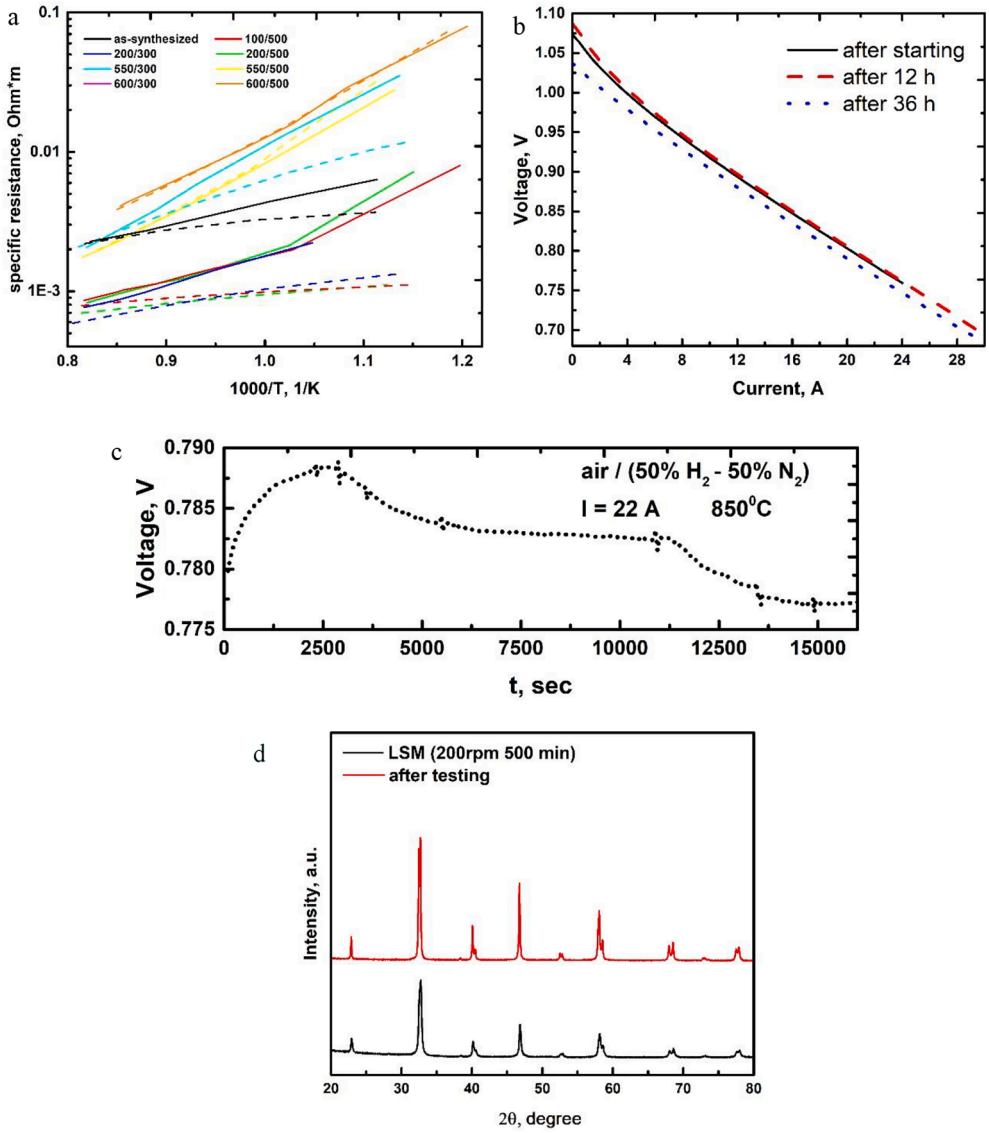

Fig.3. Specific electrical resistivity of the contact layers made of various LSM powders (a), current–voltage curves (b) and voltage vs. time dependence of the model SOFC assembled with the LSM contact layer under 22A current load (c), and XRD patterns of as-prepared LSM and LSM after testing (d). The solid and dashed lines in (a) correspond to the data collected on initial heating and subsequent cooling, respectively.

used to prepare contact paste was, therefore, ball-milled in these conditions.

Thermogravimetric analysis of the LSM paste showed that the weight of remaining manganite becomes constant on heating above at 700–750 °C (Fig. 2a). This ensures that all organic additives are completely removed prior to SOFC sealing at 940 °C. At the same time, the contact layer sintered in the course of SOFC sealing, remains sufficiently porous to provide an absence of gas diffusion limitations (Fig. 2b).

The results of electrical resistivity tests of the sintered LSM layers are presented at Fig. 3(a). The contact layers made of the powders pre-activated by grinding exhibit a higher conductivity in comparison with the layer made of as-synthesized LSM. At the SOFC operating temperatures, the difference between the corresponding values is up to approximately 3 times. In the cases when increasing ball-milling speed and/or time leads to partial decomposition of the perovskite phase, the electrical resistance becomes higher.

The current–voltage dependencies of the model SOFC after sealing and after 12 and 36 h testing under steady-state conditions are presented in Fig. 3(b). The power density at 0.7 V is 240 mW/cm^2, in a good accordance with other reports [9,14–15]. Fig. 3(c) displays time dependence of the voltage under fixed current density. In general, the use of LSM contact layer made it possible to achieve sufficiently high currents and a stable operation. Although a minor decrease in the SOFC performance was observed after 36 h, this phenomenon is clearly associated with decreasing open-circuit voltage under zero current (Fig. 3b), which suggest an appearance of small gas leakages. Microstructural analysis of the LSM contact later after SOFC tests did not reveal any significant defects like cracks or exfoliation (Fig. 2b) XRD analysis confirmed these conclusions (Fig. 3d).

4. Conclusions

Submicron LSM powder was synthesized by the glycine-nitrate technique as a precursor for contact layers between the SOFC cathodes and ferritic stainless steel current collectors. Pre-grinding treatment conditions were optimized in order to decrease grain size, to increase electrical conductivity and to enable formation of mechanically stable contact layers without use of inorganic sintering aids. Ball-milling at 200 rpm during 500 min makes it possible to achieve these goals.

Excessive rotating speeds and/or time was found to result in partial decomposition of the LSM perovskite phase, leading to worse electrical properties. Successful use of the LSM contact material without inorganic additives was demonstrated in model planar SOFC unit with the geometric area of 10 × 10 cm^2.

CRediT authorship contribution statement

E.A. Agarkova: Data curation, Investigation, Writing – original draft. **D.V. Matveev:** Data curation, Investigation. **Yu. S. Fedotov:** Data curation, Investigation. **A.I. Ivanov:** Data curation, Investigation. **D.A. Agarkov:** Writing – original draft, Writing - review & editing. **S.I. Bredikhin:** Supervision, Methodology.

Declaration of Competing Interest

The authors declare that they have no known competing financial interests or personal relationships that could have appeared to influence the work reported in this paper.

Acknowledgment

This work was financially supported by Russian Science Foundation (RSF) grant 17-79-30071.

Appendix A. Supplementary data

Supplementary data to this article can be found online at https://doi.org/10.1016/j.matlet.2021.131462.

References

[1] L. Duan, K. Huang, X. Zhang, Y. Yang, Comparison study on different SOFC hybrid systems with zero-CO_2 emission, Energy 58 (1) (2013) 66–77, https://doi.org/10.1016/j.energy.2013.04.063.

[2] H. Zhu, R.J. Kee, Thermodynamics of SOFC efficiency and fuel utilization as functions of fuel mixtures and operating conditions, J. Power Sources 161 (2) (2006) 957–964, https://doi.org/10.1016/j.jpowsour.2006.05.006.

[3] Yu. Wang, et al., Single atom catalysts for fuel cells and rechargeable batteries: principles, advances, and opportunities, ACS Nano 15 (1) (2021) 210–239, https://doi.org/10.1021/acsnano.0c08652.

[4] P. Holtappels, U. Stimming, in: Handbook of Fuel Cells, 2010, p. 75, https://doi.org/10.1002/9780470974001.f104020.

[5] I.N. Burmistrov, et al., Fabrication of membrane-electrode assemblies for solid-oxide fuel cells by joint sintering of electrodes at high temperature, J. Electrochem. 53 (8) (2017) 873–879, https://doi.org/10.1134/S1023193517080043.

[6] T.L. Wen, et al., Material research for planar SOFC stack, Solid State Ionics 148 (3–4) (2002) 513–519, https://doi.org/10.1016/S0167-2738(02)00098-X.

[7] I.N. Holtappels, et al., Preparation of membrane-electrode assemblies of solid oxide fuel cells by co-sintering of electrodes, J. Electrochem. 52 (7) (2016) 669–677, https://doi.org/10.1134/S1023193516070053.

[8] P. Holtappels, C. Bagger, Fabrication and performance of advanced multi-layer SOFC cathodes, J. Europ. Cer. Soc. 22 (1) (2002) 41–48, https://doi.org/10.1016/S0955-2219(01)00238-2.

[9] K.D. Seo, et al., Investigation the effect of current collecting conditions on solid oxide fuel cell (SOFC) performance with additional voltage probes, Int. J. Hydrogen Energy 43 (4) (2018) 2349–2358, https://doi.org/10.1016/j.ijhydene.2017.11.109.

[10] Z. Yang, et al., Electrical contact between cathodes and metallic interconnectors in solid oxide fuel cells, J. Power Sources 155 (2) (2006) 246–252, https://doi.org/10.1016/j.jpowsour.2005.05.010.

[11] W.B. Guan, et al., Effect of contact between electrode and interconnect on performance of SOFC stacks, Fuel Cells 11 (3) (2011) 445–450, https://doi.org/10.1002/fuce.201000176.

[12] M.C. Tucker, et al., Mechanical and electrochemical performance of composite cathode contact materials for solid oxide fuel cells, J. Power Sources 239 (2013) 315–320.

[13] R. Peng, et al., Characteristics of $La_{0.85}Sr_{0.15}MnO_{3-\delta}$ powders synthesized by a glycine-nitrate process, Fuel Cells 6 (6) (2006) 455–459, https://doi.org/10.1002/fuce.200600009.

[14] B. Yang, et al., Effects of slurry composition on the electrolyte support structure and performance of electrolyte-supported planar solid oxide fuel cells, Ceram. Int. 45 (2) (2019) 1528–1534.

[15] M. Ilbas, B. Kumuk, Numerical modeling of cathode-supported solid oxide fuel cell (SOFC) in comparison with an electrolyte-supported model, J. Energy Inst. 92 (3) (2019) 682–692, https://doi.org/10.1016/j.joei.2018.03.004.